ANALYSIS OF THE MAIN FACTORS THAT LED TO DEFORMATION AND CRACKING OF THE CEILINGS BETWEEN THE MINING LEVELS OF CANTACUZINO MINE - SLĂNIC SALINE

Dacian Paul MARIAN, Ilie ONICA**, Bogdan POSTOLACHI****

Abstract: *The mining at Cantacuzino salt mine, from Slanic area, began in 1993, with rooms and pillars method on multiple levels, separated by rock salt ceilings. Over time, the ceilings have suffered vertical fissures and displacements that compromised their stability. This article introduces an overview of these geomechanical aspects and a synthetical analysis of the main factors that led to shrinking stability in the ceilings between mining levels such as: the distribution of the rock salt geomechanical characteristics in the deposit, the rock salt natural cracking conditions, the native and induced stress state, etc.*
Key words: *salt rock, room, pillar, ceiling, deformation, fissure, stress*

1. Generalities

The mining at Cantacuzino salt mine from the Slanic area began in 1993. The selected mining method was small rooms and square pillars, and a flat roof between level V and VII. The same mining method was applied to start from level VIII, but with a vaulted roof [5]. The pillars width increased with the depth of mining, as follows: for levels V – VII, Lp = 16m; for levels VIII – X, Lp = 17m; for level XI, Lp = 18m (fig.1).

By 2019, it was mined about 4,964,880 tons of rock salt that resulted in roughly 2,364,229 m3 of voids. The mined spaces' depth is nearly 103 m, below a massive salt block and a layer of rock cover, which varies between 102 m and 160 m (depending on the surface topography). Considering all general data presented above, we can conclude that, concerning the stability situation, the geo-mining conditions of the Cantacuzino mine are much more favorable than those particulars of the Victoria mine and the Old mines.

Table 1 presents some comparative details (reviews from [9]) between early 2001 and 2009 on cracks and fissures that came out, in the eastern part of the Cantacuzino mine, at the hanging and footwall of the V th to XI levels. In the mapping plans of the each mining level, it can be a remark that these fissures follow a parallel boundary of the waste rocks deposit with the N-S, E-W, NW-SE, NE-SW, and N-S direction (fig.2).

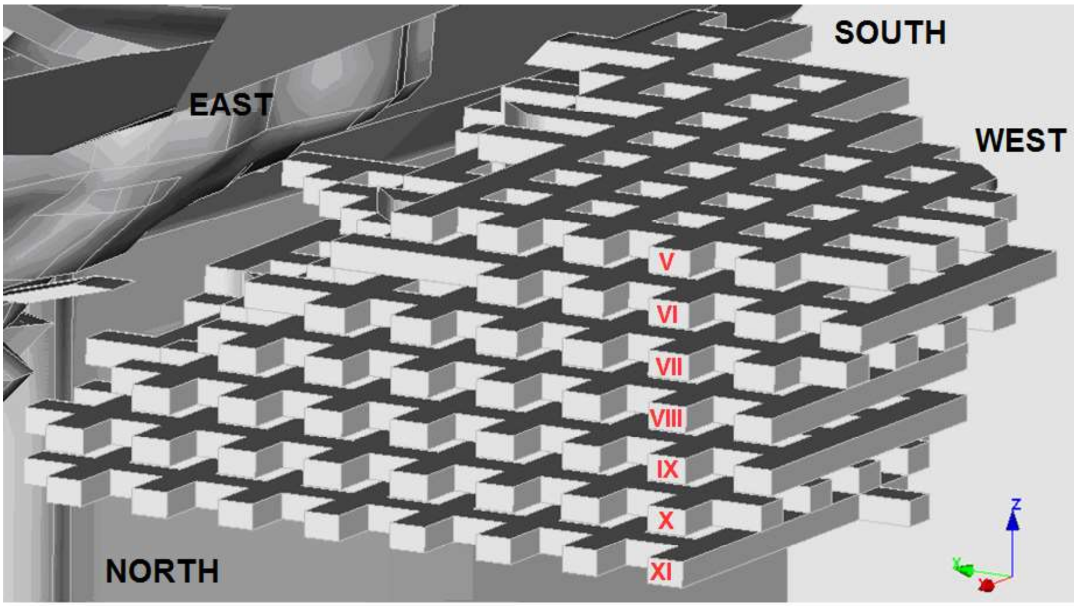

Fig.1. *3D view of the Cantacuzino mine [7]*

** Lect.eng. Ph.D, University of Petroșani*
*** Prof.eng.habil. Ph.D, University of Petroșani*
**** Eng. Ph.D stud., University of Petroșani*

Table 1. *The comparative situation of fissures between 2001 and 2009 [7]*

Level	Start of mining	Crack orientation	Floor		Roof	
			2001	2009	2001	2009
Level V +289 m	1992	The affected area, in m^2	1350	2925		1350
		N-S				
		E-V				
		NV-SE				
		NE-SV				
Level VI +273 m	1994	The affected area, in m^2	3600	5700		3000
		N-S				
		E-V				
		NV-SE				
		NE-SV				
Level VII +257 m	1996	The affected area, in m^2	750	4000	1650	4050
		N-S				
		E-V				
		NV-SE				
		NE-SV				
Level VIII +241 m	1997	The affected area, in m^2	1500	7650		3875
		N-S				
		E-V				
		NV-SE				
		NE-SV				
Level IX +225 m	1998	The affected area, in m^2		3300	225	875
		N-S				
		E-V				
		NV-SE				
		NE-SV				
Level X +209 m	2003	The affected area, in m^2				
		N-S				
		E-V				
		NV-SE				
		NE-SV				
Level XI +193 m	2005	The affected area, in m^2				
		N-S				
		E-V				
		NV-SE				
		NE-SV				

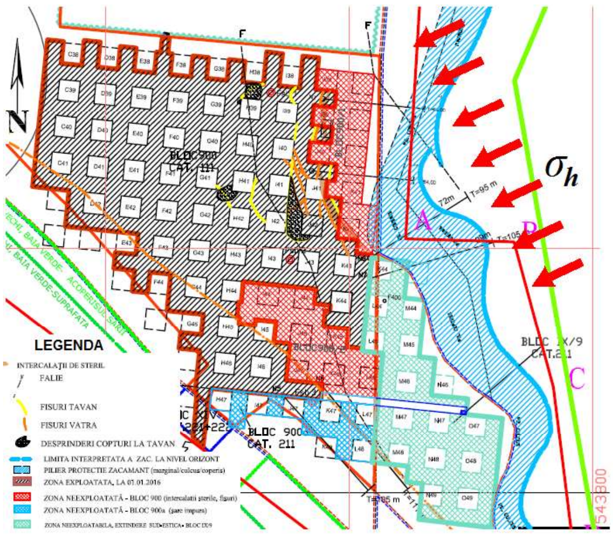

Fig. 2. *Development of maximum horizontal stresses, from E - (N-E) direction, in the Slănic Prahova rock salt deposit, at level IX (+225m) [7]*

The monitoring progress of cracks / fissures, by topographic and other measurements was performed, between the V th and XI th levels, periodically and recorded the value of horizontal and vertical displacements based on some benchmarks. Therefore, there were recorded four-fault systems, with N-S, NW-SE, E-V, NE-SW orientation with approx. 45o angles between them and variable lengths, from the ceiling by ceiling, ranging between 20 m and 150 m.

Inspecting the data from table no.1 it can be concluded that the whole area affected by cracks and fissures in 2009 increased by almost 4 times, compared to 2001. That statement can be defined by the constant distribution of the stress around the mining excavations, and the attending factors such as humidity mining pressure and the regular impact of seismic waves generated by blasting operations have contributed to the salt degradation.

The investigation of cracks and fissures that showed out in the strength structures (especially in the ceilings between levels) in the case of the Cantacuzino mine was also performed with the aim of electrometric measurements ([2], [10], [11]) at VIII, IX and X levels.

To find out the origin of the cracks and fissures developed in the ceiling roof at levels V-IX, we need a detailed analysis of their positioning towards the marginal pillars. It is also crucial to know the fissures' size and orientation, the distribution of geomechanical rock salt characteristics, the stress state, and the ceiling deformations between multiple levels. The factors taken into account could have contributed to the appearance of fissures in the ceilings. With a precise location and geometry which respect approximately the same model, at all levels, are known the followings:1) The rock salt quality, with weaker geomechanical characteristics, from the areas which are damaged by cracks and fissures; 2) Stress distribution as an outcome of underground mining; 3) Arising of some specific characteristics of rock salt during its genesis between the rock salt body and waste rocks [7].

2. Description of the destabilization phenomena of the ceilings from the Cantacuzino mine generated by the presence of fissures

The stability of continuous rock salt ceilings depends only on the limit strength achievement of various geomechanical characteristics of rock salt by (tensile, shear, compressive) strength generated by their bending phenomena. Perhaps, in the ceilings affected by failures, the floor strain leads to the mobilization of their strength characteristics (cohesion, internal friction angle, shear and tensile strength, etc.) of these low resistance plans.

In the case of continuous rock salt ceilings, for stability analysis can apply the cylindrical plate bending theory. When the floor thickness between mining levels exceeds 1/5 of the room width, the situation is introduced above (when the ratio may exceed 1/2) as a result, the theory of plates is no longer relevant. The effect of shear force, neglected in the classic thin plates theory, becomes essential in thick plates. Therefore, both the bending moment and the shear force are involved in the generation of vertical displacement / subsidence of the ceiling. The calculation of bending moments and shear forces and their strength respects the theory of thick plates. The failure are generally manifesting in thick plates by shearing cantilever plates or slipping their structure along the vertical fissures [12].

Based on the theoretical elements and research results encountered in practice, presented in the literature and also, regardless of the database obtained from observations made on ceilings' stability between mining levels, from the Cantacuzino mine, further, we will describe some typical phenomena of these ceilings stability.

2.1. Ceiling displacement by an inclined fault

Is the general case, presented teoretically by Benyakhlef [1]. The geomechanical phenomenon is an argued by the vertical displacement measurements based on the landmarks laid out on the ceilings between each mining level, namely the negative vertical displacements, with low values, up to -20 mm, which express swelling of the floor at the measured points level. Being about natural dense structures, loaded gravitationally by their weight and equally distributed on the floor surface, is oriented to move downwards. An upward displacement can occur only when, during its vertical movements, the rock salt massive encounters some reactions that causes it to change its vector displacement direction.

The ceiling between levels is embedded, inside the marginal pillars, and above each mining pillar. It is vertically loaded by own weight $\sigma_v = \gamma \cdot h = 2.1 \cdot 8 = 16.8$ tf/m² ($\gamma = 2.1$ tf/m² – density of rock salt; h=8m - ceiling thickness) and by horizontal stress developed by rock salt massive along the $\sigma_{hp} = k_{pl} \cdot \gamma \cdot H$ (H is the ceiling depth, measured from the surface; k_{pl} is a concentrator of horizontal stresses σ_h distributed in the ceiling).

The stresses concentrator has the following value:

$$k_{pl} = \frac{(h_c + h_{pl})}{h_{pl}} \cdot \frac{\nu}{1-\nu} = \frac{8+8}{8} \cdot \frac{0,28}{1-0,28} = 2 \cdot 0,39 = 0,78$$

where: h_c is the room height; h_{pl} – ceiling thickness; ν - Poisson ratio.

Even though the horizontal stress is about 39% from vertical stress, geological and geomechanical information suggests approaching vertical stress value. As a result, this k_{pl} ratio of compressive stresses in the ceiling is close to 1.5-2.

In swellings presents in the floor, the phenomena is explained by the lower block subduction below the upper one. The blocks are separated by a fault from the ceiling structure, with a certain tilt towards the vertical (fig.3). With the higher tilt of the plane, the more intense compressive stress is present in ceilings. The strength characteristics of fault are lower; thus, the floor swelling is more significant. Because of insignificant negative and positive vertical movements of the ceiling and due to the compressive stress that involves the separated blocks to stay connected, the fault which is present in ceiling structure is not dangerous for stability, unless there are other fractures in the surroundings, which produce local de-stressing phenomena as well as blocks that can move freely under gravity (see fig.5).

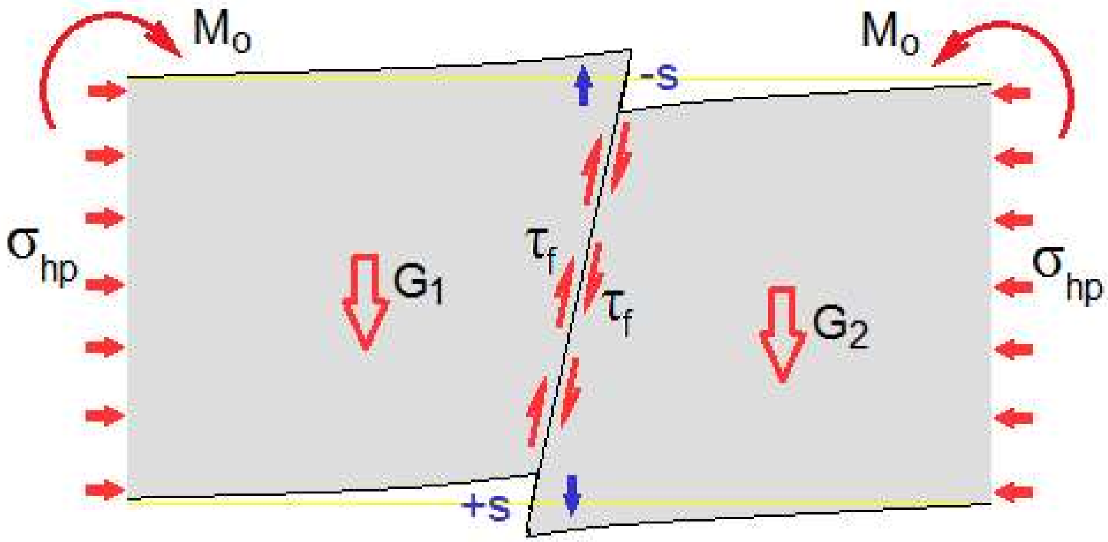

Fig. 3. *Ceiling loss of stability caused by an inclined fault [7]*

2.2. Ceiling displacement by a vertical fault

The theoretical models presented by Benyakhlef [1] represent ceilings (plates) crossed by an inclined fault towards the vertical with the angle $\theta \neq 0^o$. For a similar situation but with angle $\theta = 0^o$, it presents a vertical fault, shown below.

From a theoretical point of view, this case is similar to the one presented in point 2.1. However, the loss of stability phenomenon is slightly different. Under the detached blocks' stress own weights G_1 and G_2 with their compressive strength, there are present bending and shear stress in the ceiling that cause vertical movements $+s$. After vertical displacements, the two blocks separated by the vertical fault spin around the boundary edge A so that the horizontal shrinking forces are concentrated in a very narrow area. Which leads to high stress that exceeds the strength of the rock salt mass. This results is breaking off contact edges. The phenomenon causes subsidence to increase. Theoretically, the ceiling turns from a cantilever plate into the shape of two plates in the console. At this stage, the strain is much more critical at the cantilever level, which leads to blocks failure at the edges of the pillar, followed by their total detachment from salt massive and the increase of vertical displacements. The detached blocks behave like two articulated blocks at the edges A, B, and C, loaded by friction forces and their weight concentrated in those three hinges. Due to the stress concentration in these areas, over time, the destruction of their contact corners is inevitable, leading to an acceleration of the ceiling collapse.

In conclusion, until the collapse point is reached, a ceiling crossed by a vertical fault passes through the following three stages: 1) embedded plate, which is bends under a distributed force; 2) two cantilever plates loaded for bending, with one hinge (fig.4.a); 3) two detached blocks, articulated with three hinges (fig.4.b).

This phenomenon is less likely to occur after a relatively short period, and if it takes place, it will occur in a long period after the ceiling is build. Due to lateral stress σ_{hp} with high values that manage to keep the blocks in touch, they work as a homogenous structure.

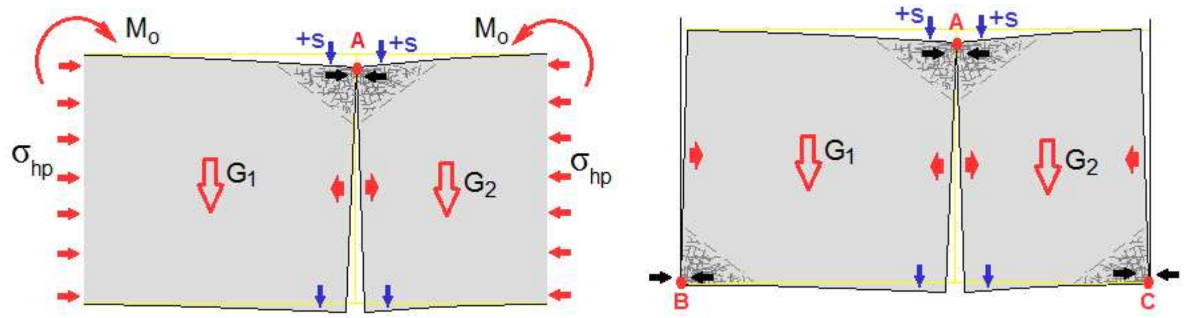

a) **b)**

Fig.4. *Ceiling loss of stability caused by a vertical fault [7]*
a) ceiling with a hinge; b) ceiling with three hinges

2.3. Dislocation of the ceiling by two or more fractures

Analyzing the ceiling's mapping plan from the Cantacuzino mine (see fig.2), it can be noticed that towards the eastern area, the ceiling is affected by a system of roughly parallel fractures, extended over different lengths and with different amplitudes. Compared to the situations presented above, the ceiling structure of two or more close fissures is more frequent. Also, in the way they affect the stability of the ceiling, they are much more dangerous.

When two fractures cross a ceiling, the loss of stability is based on the fractures' mutual inclination and the vertical inclination. Their mutual inclinations may be parallel (vertical and inclined), convergently inclined towards the ceiling, or divergent.

From the types of fractures described above, the most dangerous ones have convergent inclinations towards the ceiling because they allow the gravitational separation of intermediate blocks from the ceiling structure, leading to inevitable collapse (fig.5.a). The more significant divergence of angles increases the risk of ceilings displacement.

The ceiling collapse phenomenon starts with its initial bending strain, generated by the reunion of its weight and lateral stress forces. As vertical displacement increases, inside the ceiling come out the bending moment that causes detachments by necking of craking planes, driven by shears generated from the gravitational shifting of the intermediate blocks. The variable characteristics from the minimum stress plans and the salt blocks' non-homogeneous structure came out some strain concentrators in their structure and horizontal breaks, leading to fragments detachments between fissures rooms roof at lower levels. Separation of a salt volume from the ceiling structure leads the horizontal stresses to load a more reduced ceiling thickness. The critical moment is reached when the ceiling thickness is reduced as more the stress and displacement increase—further followed by detachments of new volumes of rock salt from the central block. Finally, it ends with the total collapse of the central block and penetration of the ceiling. Next, the phenomena that cause the collapse of a failure ceiling occurs based on the particular geomechanical conditions around the sinkhole.

If the conditions presented above determine an intermediate risk of instability, then the existence in the ceiling of three or more approximately parallel fractures increases its vulnerability level in terms of the collapse (fig.5.b). These location conditions of a ceiling generate the highest risks of stability lost and subsidence. Even if the peripheric fractures' inclinations are convergent towards the ceiling, the third or fourth intermediate fracture's presence makes the destruct of the intermediate block possible in a much shorter amount of time (fig.5.b).

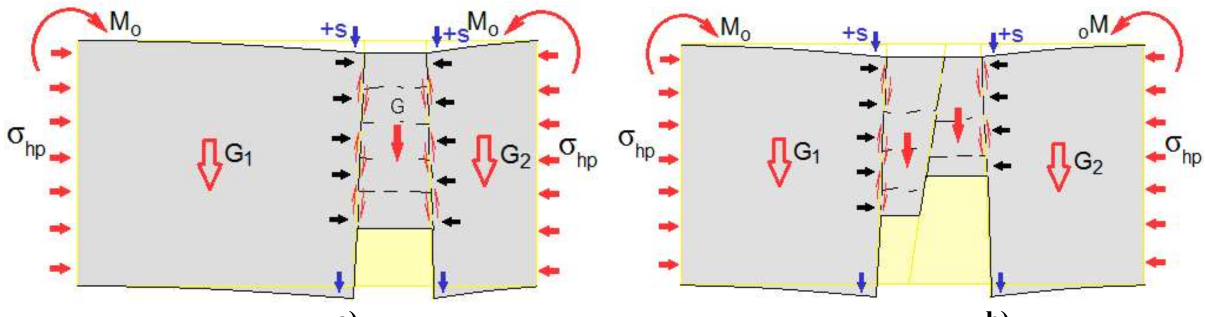

a) **b)**

Fig.5. *Ceiling loss of stability caused by two or more close faults [7]*
a) collapse of the ceiling following two faults; b) collapse of the ceiling following three faults

3. The quality of the rock salt in the areas affected by fissures / cracks

After the analysis of the geomechanical data presented in the following works ([7], [9]), it can be concluded that, in general, the values of the geomechanical characteristics of rock salt samples, taken from affected areas by the fissures and faults are within the limits of their range of variation, at each mining level, with a tendency towards the average values of the domain.

Also, there is an apparent separation of geomechanical characteristics by types of rock salt (crystalline white and dark-grey) and is claimed a decrease (up to 50%) for crystalline white rock salt located in the ceilings affected by fissures at Cantacuzino mine.

The same thing can be concluded from the analysis of geomechanical characteristics, investigated on white and purple samples of rock salt, taken from the upper areas of the deposit (probably from the Unirea mine) by Prof. Stamatiu ([16], [17]).

The above statement can assume that weaker geomechanical properties of white rock salt from areas affected by the cracks and fissures may be a factor that contributes more to the size of these dislocations. Their growth and genesis are mainly determined by other important factors, such as those related to the state of stress. They will be analyzed in further.

4. Distribution of stress concentrators, as a result of underground mining excavations

The stress in the rock mass is grouped, depending on the origin in *the natural state of stress*, discovered in the intact rock masses and *induced stress* resulting from rock masses loading by mining and civil excavations [3].

Gravitational stress result from the rock weight on the surface unit, above a point of earth's crust. To calculate the vertical component, you can write [3]:

$$\sigma_v = \int_0^z \rho \cdot g \cdot dz$$

where: ρ average apparent density of the rocks; g - gravitational acceleration; z – the depth measured from the surface.

The natural state of stress $[\sigma_o]$can be considered a geostatic or gravitational one, represented by the vertical geostatic stresses $\sigma_v = \rho_a \cdot g \cdot H$ and horizontal geostatic stress $\sigma_{h1} = \sigma_{h2} = \frac{\nu}{1-\nu} \cdot \sigma_v = k_o \cdot \sigma_v$; where: $k_o = \frac{\nu}{1-\nu} = \frac{0.28}{1-0.28} = 0.39$ ν is the Poisson ratio.

The excavation presence's induce stresses $[\sigma_e]$ are the tractions on inside surfaces of the excavations represented by the horizontal σ_{eh} and vertical σ_{ev} stress. The loading of the model was performed in total stress: $[\sigma_T] = [\sigma_o] - [\sigma_e]$.

In the paragraph above was presented the theoretical term of *natural* and *induced stress*. However, the natural state of stress includes gravitational and tectonic stress the residual and geothermal stress [3]. Therefore, in order to establish the right values of *natural stress* of Slănic Prahova rock masses conditions, it has been necessary to carry out in situ rock stress measurements through several known methods, such as: hydraulic fracturation, use of flat jack, overcoring, etc. ([4], [15]). The assessement of natural stress state from in situ measurements would have led to a better description of the phenomena that caused the cracks and displacements in-room ceilings at the Cantacuzino mine.

The natural geostatic stresses (vertical and horizontal) are calculated according to the relations presented above. The results from all mining levels at the Cantacuzino mine are presented in table 2.

Table 2. *The natural state of stress calculated in the floor of each mining level from the Cantacuzino mine[7]*

Level	Floor level, m	Depth, *H*, m		Vertical stress, σ_v, $\cdot 10^4$ N/m^2		Horizontal stress, σ_h, $\cdot 10^4$ N/m^2	
		max.	*min.*	*max.*	*min.*	*max.*	*min.*
Level V	+289	186	111	390,6	233,1	152,334	90,909
Level VI	+273	202	127	424,2	266,7	165,438	104,013
Level VII	+257	218	143	457,8	300,3	178,542	117,117
Level VIII	+241	234	159	491,4	333,9	191,646	130,221
Level IX	+225	250	175	525,0	367,5	204,75	143,325
Level X	+209	266	191	558,6	401,1	217,854	156,429
Level XI	+193	282	207	405,3	434,7	158,067	169,533

The volume of stress induced by the mining operations in the support structures (pillars and ceilings) is directly proportional to the volume of empty spaces created from rock salt mining. Therefore, we can remark that the state of stress and strain of rock salt mass have increased according to the depths because of deep mining. Moreover, if we follow data of the most affected areas by cracks and fissures in the ceiling at each level (table no 1), it is obvious that the most affected mining levels are those in the center of the Cantacuzino mine, mostly at the level VI, VII and VIII, which point out a high-intensity area of vertical stress, emphasized by the time factor.

Taking into account the effects of induced stress distribution on ceilings, we can notice the most popular stability analysis theories are based on the hypothesis of bending plates [12], where rocks are presented as elastic, continuous, and isotropic environments. Calculations are performed in the plane strain or plane stress hypothesis.

In the above paragraph, we present a graphical model (fig.6), where ceilings are assumed to be flat embedded plates and elastically supported by the inter-room mining pillars. In this model, the pillars are replaced by some springs, whose behavior is run by the law $\{F\} = -K \cdot \{u\}$ (where: K is the pillar rigidity; $\{F\}$ - reaction forces of the pillar; $\{u\}$ - vertical displacement of the pillar).

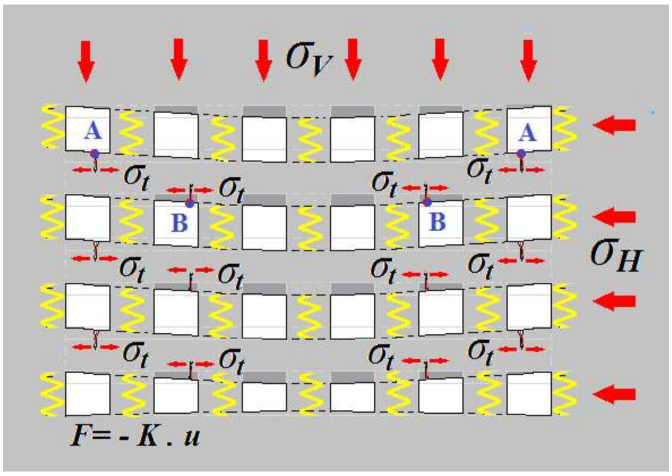

Fig. 6. *Figurative model of the resistance structures (pillars and ceilings) from the Cantacuzino Mine, based on the cylindrical bending theory of flat plates [7]*

The ceilings between mining levels, represented in figure 6, due to the stresses caused by their weight combined with the horizontal stress, formed in the rock salt massive, over marginal pillars, will suffer both horizontal and vertical displacements. These can be highlighted in the numerical models created for stress and strain analysis in the Cantacuzino mine case. The distribution of displacements at the mining levels is lower at the edges of active mining areas and more accentuated towards the mined space center.

As shown in the figure mentioned above, the maximum bending moment is at the level of ceiling embeddings, in the marginal safety pillars. Theoretically, this should have the maximum tensile stresses to appear at the embeddings, accordingly the wall, on the ceiling's upper surface (floor). However, on the opposite side, should appear maximum compressive stress at the roof base.

If we analyze the mapped fissures (see fig.2), the floor's fissured system is located at a certain distance from the marginal pillars (and not at their boundary). The roof' fissures system has the same orientation but is located on the second strip, a little further away, towards the center of the mining level. In the model from figure 6, two inflection points are noticed: present compressive stress, one in the floor level point A and another in the roof level point B.

Removal of fracturing strips to the mining center towards the mining center suggests that the ceiling structure's failure, by tensile stress, did not occur due to exceeding the rock salt resistance limits but due to the dislocation of pre-existing planes of minimum resistance in the rock salt deposit structure. This phenomenon is also described by the failure criteria presented below.

In terms of analytical models based on the cylindrical bending theory of flat plane (figure 7), are distinguished the following stability cases of plates/ceilings which are under the influence of underground excavations ([13], [14]). So, according to stress occurring in the plates structure, subject to the complex loading, there were recorded to their resistance characteristics, the following stability conditions:

a) if $\sigma_{min} < 0$ - opening the fissures;

b) if $R_{ultima} \leq \sigma_{max} \leq R_c$ - the failure of the rock in time;

c) if $\sigma_{max} \geq R_c$ - instant failure.

Analyzing the failure conditions of stability presented above shows that the Cantacuzino mine's ceiling fits with the first case of strain. That leads to the opening of pre-existing natural cracks, according to the case represented in fig.7.b.

On the western side, contrary to the cracked region, at the boundary limits of mining levels, are no cracks caused by a bending moment of ceilings or from other moments. This statement leads us to the idea of presence towards the eastern area of some natural fissures, which acts independently from the loading caused by excavations that were left from rock salt mining operations.

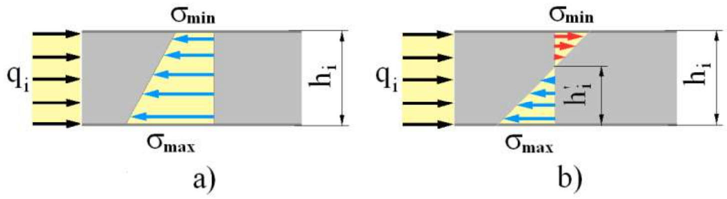

Fig.7. *Development of the state of strain in a plate (beam) the subject of complex bending - bending and buckling ([13], [14]) a) compressive stress; b) compressive and tensile stress*

5. Genesis of natural / pre-existing fissures in the eastern part of the deposit

The rock salt deposit from Slănic Prahova has a lenticular shape with a length of approx. 2 700m to the north-south, the width of the lens is between 800m and 2300m, and the maximum thickness is 499m, in the central area.

Based on tectonics, the deposits from the Slanic area are located in a sizeable Miocene syncline (Slănic syncline), being located in the northern part over the Paleogene formations of the Homorâciu spur. The rock salt in the middle of the syncline is intensely fractured because of the Homorâciu anticline's lateral pressure.

In the central-northern area of the deposit, we can notice the presence of diapirism, where the rock salt deposit is penetrating the overlying Badenian deposits, because of lateral pressures that loaded the rock salt deposit.

The mining works evidenced the salt body's laminations towards its margins, presenting marl - clay interstratifications, especially at the salt - sterile boundary.

Considering the geological information presented above, we try to represent the genesis of natural fissures that arose towards the eastern part of the salt massive, using the picture model in fig.8.

Fissures were affecting the ceiling in the eastern area of the deposit, at the border with the marginal pillar. They have been driven to salt massive or are results of a primary dislocation of pre-existing natural fissures, both generated by tensile and shear strain, developed under the loading of resistance structures due to mining perturbations.

In the previous point, we presented the elements that deny fissures, which result in intact salt massive failure. Therefore, in the following, we will claim the rock salt massive of some structural and micro tectonic faults, manifested as a result of orogenic loadings.

As shown in Figure 8, the deposit is subject to a natural state of geostatic stresses $\{\sigma_V, \sigma_H\}$, added, among other stress generated by orogenic loadings $\{\sigma_{SO}\}$. The development of orogenic loading *SO* in the eastern part of the deposit was after the formation of the Slănic rock salt lens. This is suggested, among other information, by its flattened shape towards the eastern part, at the boundary with the sterile rocks. We should consider the shape of the 3rd zone, from figure 8. The vector of maximum displacements has an inclination of almost 40-45^o from the horizontal plane, with an amplitude of approx. 40-60m. The values of the maximum lateral stress $\sigma_{h\,max}$ are present in table 2.

Considering their group direction, the fissures developed in ceilings between mining levels can be concluded that the orogenic strains' direct result was lamination and collapse of rock salt masses at the boundary between salt and sterile rocks shown in the dispersion zone 4, larger than 50-60m. This phenomenon was made possible by the different behavior of the surrounding sterile rocks, which is a rigid-elastic one, compared to the elasto-plastic towards the rock salt mass's visco-plastic behavior. Furthermore, the orogenic strains' stress is spread in the rock salt massive in plastic deformations, which proceed with structural displacements in zone 4, at the eastern boundary between the salt mass and sterile rocks. The direction of these displacements follows the eastern surface's shape that sets out the contours between rock salt massive and surrounding rocks.

According to information achieved from geoelectric measurements, came out the idea of a „strain area" (specific to nature massive [4], [15]) present at the eastern limit of the Cantacuzino Mine. This is not obvious due to the spread of orogenic energy in plastic deformation and micro tectonic displacement, in the 4 th zone and partially in 3 rd zone.

The cracks and fissures phenomenon described above is also reviewed in other publications [6]. This paper notes that horizontal stresses can cause buckling and failure in roof and ceiling rocks. In this case, the displacement follows a lateral propagation trend in a perpendicular direction to the primary horizontal stress and can wave through the mine, as shown in figure 9.

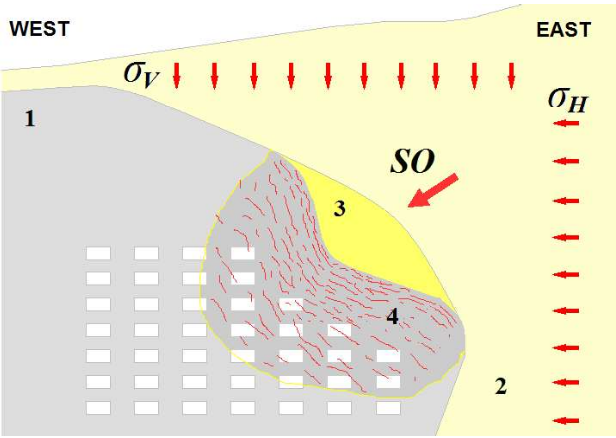

Fig. 8. *Formation of the natural fissured area in the rock salt deposit from Slănic, Cantacuzino Mine, as a result of orogenic stress [7]*
1- the rock salt deposit; 2- the surrounding sterile rocks; 3- the area of orogenic displacement; 4-fissured area SO-orogenic loading; σ_V şi σ_H - vertical and horizontal natural stress

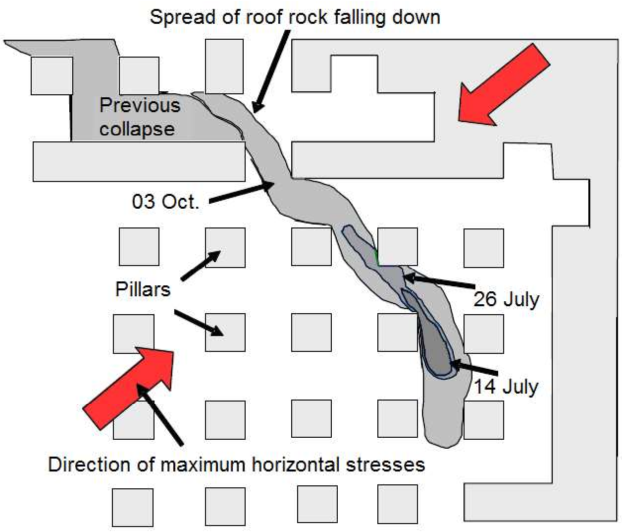

Fig. 9. *Plan view with the development of the stress correlated with the ceiling failure in a direction perpendicular to the maximum horizontal stress [6]*

Careful observation of roof and ceiling displacement, their direction of propagation, and other indications of excessive stress on the rock salt massive can help identify maximum horizontal stress [8].

Comparing the phenomenon and the collapse model of ceilings, generated by excessive horizontal stress, shown in figure 9 by (Iannacchione and others) [6], and the fractured zones' condition in figure 2, typical for Cantacuzino mine, one figurative similarity should be considered. Another argument in favor of fissures genesis is enormous lateral stress from the eastern part of the salt massive from where it can be concluded.

6. Subsidence measurements analysis of the ceilings in the case of Cantacuzino Mine

In order to monitor the vertical displacement of ceilings from Cantacuzino mine, there were established several topographic benchmarks. The high-precision topographical measurements were made yearly, beginning with the year 2009. The benchmarks were set along alignments in the areas of interest, in the places with the most accentuated vertical displacements or ceiling failures, as following: at the 5 th level, 13 benchmarks installed on 1 st alignment; at the sixth level, 26 benchmarks on 3 alignments; at the 7 th level, 34 benchmarks on 6 alignments; on the 8 th level, 39 benchmarks on 5 alignments; at the 9 th level, 32 benchmarks on 5 alignments; at the X th level, 25 benchmarks on 5 alignments.

The different estimation functions (linear, logarithmic, and power) of the measured values are summarized in table 3. The benchmark with the highest sinking speed at each level demonstrates the variety of geomechanical behaviors and the different ceilings subsidence phases. Sinking speeds show both the evolution phase of the ceiling deformation and the most vulnerable points (benchmark) in terms of stability lost.

From table 3, it can be concluded that the most considerable cumulated subsidence at the level of each ceiling correlates with the highest sinking speeds, which leads us to the idea that the highest value of subsidence selects the benchmarks to represent the area where ceilings encounter the possible instability.

The evolution in time of subsidence (fig.10) was achieved by estimation of measurements on each selected benchmark. In general, the estimation functions are only power, for levels V-VIII th, power and linear type, for level IX and only linear, for level X. Based on this assumption, we can notice a transition of the ceiling behavior from a power law at the first 4 levels to a linear law at the last monitored level, passing through a level with both behavior types.

Table 3. *Subsidence and vertical displacements speed approximation of ceiling between mining levels [7]*

Level	Bench mark	The approximation law	Approximation formula of subsidence speed $S_{S(t)}$, mm/month	Determination factor, R^2	The last subsidence speed, mm/month	Total subsidence, mm
V	**12**	*linear*	$V_{S(t)}^{V} = -0{,}0025 \cdot t + 2{,}1452$	0,8464	1,6144	289,9
VI	**19A**	*logarithmic*	$V_{S(t)}^{VI} = -0{,}166 \cdot \ln t + 2{,}481$	0,6202	1,6532	298,6
VII	**11**	*power*	$V_{S(t)}^{VII} = 118{,}18 \cdot t^{-0{,}805}$	0,9972	1,8575	335,5
VIII	**21A**	*power*	$V_{S(t)}^{VIII} = 0{,}6931 \cdot t^{0{,}2117}$	0,7358	1,9466	351,6
IX	**33A**	*logarithmic*	$V_{S(t)}^{IX} = 0{,}9301 \cdot \ln t - 3{,}3915$	0,9527	1,3769	248,7
X	**17**	*logarithmic*	$V_{S(t)}^{X} = 0{,}2189 \cdot \ln t - 0{,}7332$	0,8105	0,297	40,7

Note: $V_{S(t)}$, mm/month; *t*, months

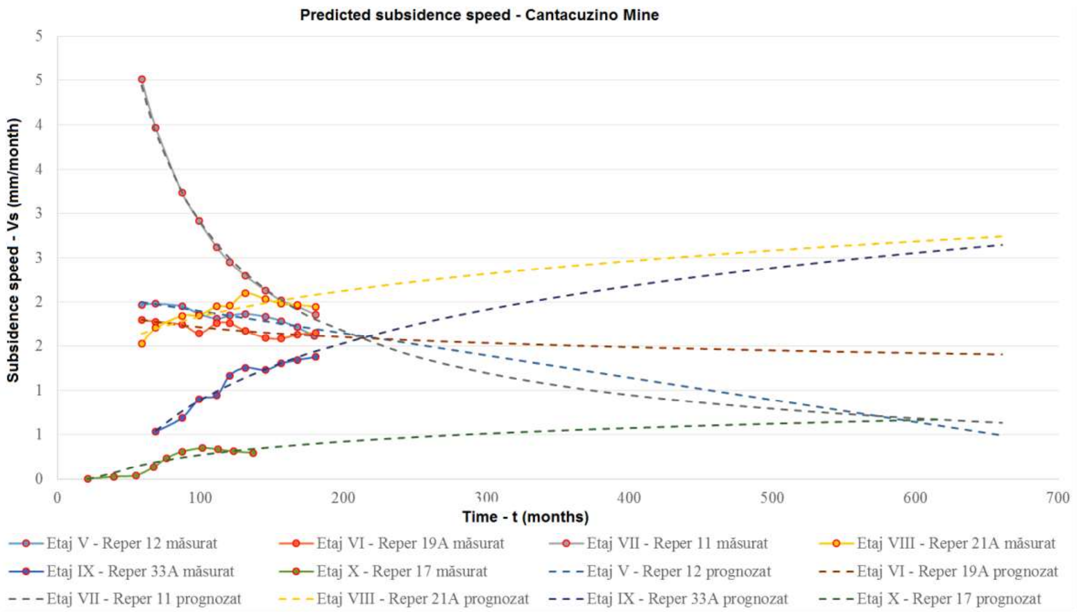

Fig.10. *The evolution in time of the predicted sinking speed at the V-X th levels, for the benchmarks with the highest value at the last subsidence measurement [7]*

The deformation phenomena that led to floor swelling were described in the second point (fig.3). We can notice from the tables with the subsidence and displacements data measured over time that these benchmarks have negative values, from the first to the last measurement. That proves the existence of a constant behavior at the benchmark level, which can be explained by the outlined form (fig.3).

From the database analysis, several indicators have suffered both from sinking and swelling of these phenomena at the floor level, mainly recorded on IX th and X th floor and less on the VIII th floor. Therefore, at the level X th, almost all the benchmarks at the first measurement recorded swellings (negative vertical displacements). Two benchmarks suffered swelling at the first 3-5 measurements, and three others passed successively through oscillating phenomena of swelling, sinking, and swelling. At IX th level, similar oscillating phenomena could be observed. For two benchmarks, the first measurements revealed sinking, then swelling of the level floor, and for the other four were notice in first swelling, then sinking. At the eighth level, only one benchmark has gone from swelling to sinking.

The statement preset above can highlight the complexity of deformation phenomena in ceilings, especially in those at the lowest levels. From the analysis with finite elements ([13], [14]) results that, due to deep mining at the Cantacuzino mine and other factors, the strength structures related to the lower level are at risk of deformation, which involves positive vertical displacements after the *y*-axis (swellings, which in this case are marked with the + sign), with values that increase in depth, from the VIII to the XI level, as in fig.11.

This scalar representation of vertical displacements could explain to some the phenomena described above. Deviations from reality are generated because the salt mass was considered continuous, homogeneous, and isotropic in numerical modeling, but in situ, it is non-homogeneous, anisotropic, and discontinuous (crossed by faults). That is why, at the levels VIII-XI, there are these intermediate phenomena of random behavior, between subsidence and swelling. The explanation may also be driven by the presence of fissures in the ceilings. In the first stage, they are stable, followed by displacements and stress relieving. Then, under recalibration and finally, the swellings turn into subsidence under the influence of their weight (collapse).

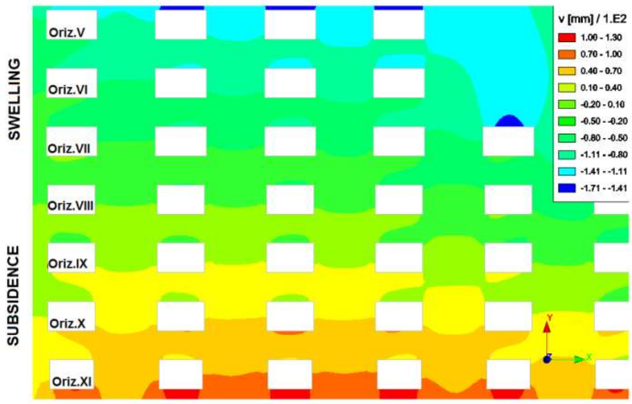

Fig.11. *Scalar representation of vertical displacements in a 2D model with finite elements, Cantacuzino mine [7]*

7. Conclusion

The Cantacuzino rock salt mine mining method was, with rooms and square pillars, on seven levels separated by the ceilings. This method was used at all salines in Romania. In almost three decades of mining operation, as continuing with mining in depths. The ceilings between mining levels suffered vertical displacements (sinking and lifting) also came out a fissure system, which led to a decrease in stability and the local collapse of ceilings.

After the macroscopic observations and the electrometric measurements, each ceiling set of fissures was discovered, oriented over the boundary of the eastern marginal pillar of the salt deposit. The risk of local collapses is influenced by the number of parallel faults (fissures), their geometry and geomechanical characteristics, the stress state, and the maximum horizontal stress vector orientation. Furthermore, both general stress state and the fissures characteristics contributed mainly to the values and distribution of vertical displacements, determined by measurements as subsidence for the upper levels and lifts for the lower.

The main factors analyzed in this article, which contributed to the appearance of fissures in the ceilings between mining levels, are the following: the quality of the rock salt, the distribution of stress concentrators, the genesis particularities of the rock salt deposit, et al.

References

1. Benyakhlef, R. (1983)
Etude des mécanismes du foudroyage, Thèse, Paris.

2. Berchimiş,S. ş.a. (2004)
Identificarea fracturilor şi fisurilor din mina Cantacuzino şi Unirea prin metode geofizice; Etapa I – mina Cantacuzino, Etajele VIII, IX, X, SC IPROMIN SA, Contract 16079/2004.

3. Herget, G. (1988)
Stresses in rock, Balkema.

4. Hirian, C. (1981)
Mecanica rocilor, Editura Didactică şi Pedagogică, Bucureşti.

5. Hirian, C., Georgescu, M. (2012)
Stabilitatea salinelor vechi din România-condiţie a utilizării lor pentru diverse domenii, Editura Universitas, Ediţia a II-a, 2012.

6. Iannacchione, A.T., Marshall, T.E., Burke, L., Melville, R., Litsenberger, J., (2003)
Safer mine layouts for underground stone mines subjected to excessive levels of horizontal stress. Min Eng 55(4):25–31.

7. Marian, D.P, Onica, I., Georgescu, M., Cozma, E. ş.a. (2019)
Studiu privind stabilitatea construcțiilor și terenului din perimetrul de influență al minelor vechi (Ocna din deal și Ocna din vale), Victoria, Unirea și Cantacuzino funcţie de datele de cunoaștere existente (topografice, reologice, geologice, hidrogeologice, etc.) precum și a deformațiilor elementelor de rezistență ale excavațiilor subterane din mina Cantacuzino, în vederea desfășurării în condiții de siguranță a exploatării și a protejării obiectivelor civile și industriale, Universitatea din Petroșani, Contract nr. 186/15.10.2019.

8. Mark, C., Mucho, T.P., (1994)
Longwall mine design for control of horizontal stress. In: Mark C, Tuchman RJ, Repsher RC, Simon CL, eds. New Technology for Longwall Ground Control. Proceedings: U.S. Bureau of Mines Technology Transfer Seminar. Pittsburgh, PA: U.S. Department of the Interior, Bureau of Mines, SP 01–94, pp. 53–76.

9. Milea, M. ş.a. (2009)
Studiul parametrilor fizico-mecanici și reologici ai sării geme din zăcământul Slănic Prahova și redimensionarea elementelor structurilor de rezistență (pilieri-planșee) a zonelor aflate în exploatare (mina Cantacuzino), în scopul asigurării stabilității de ansamblu a zonei, Etapa II/Partea 1 – Prelucrarea statistică a datelor rezultate din încercările de laborator, SC MINESA-ICPM SA Cluj-Napoca, Contract nr.10 848/2011/26.10.2007; Simbol proiect 49-724-01.

10. Oancea, I. ş.a. (2006)
Monitorizarea subsidenţei miniere la minele de sare prin metode de tomografie geofizică în vederea evitării fenomenelor de colaps. Faza II: Investigarea prin metode de tomografie geofizică a pilierilor şi planşeelor – faza I (Rezumat), INCDMRR Bucureşti, iulie.

11. Oancea, I. ş.a. (2007)
Măsurători electrometrice şi studiu geofizic pentru investigarea zonelor de slăbire structurală în orizonturile VIII, IX şi X ale minei Cantacuzino, SC IPROMIN SA, Contract 1946/22.03.2007.

12. Onica, I. (2006)
Stabilitatea excavaţiilor miniere subterane executate în medii stratificate, Editura Universitas, Petroşani.

13. Onica, I. (2016)
Introducere în modelarea cu elemente finite. Stabilitatea excavațiilor miniere, Ed. Universitas, Petroșani.

14. Onica, I., Marian, D.P. (2016)
Aplicaţii ale metodei elementelor finite în analiza stabilităţii terenurilor şi structurilor subterane, Ed. Universitas, Petroşani.

15. Popescu, Al., Todorescu, A. (1982)
Mecanica rocilor în minerit, Editura Tehnică.

16. Stamatiu, M. (1962)
Mecanica rocilor, Editura Didactică şi Pedagogică, Bucureşti.

17. Stamatiu, M. (1959)
Problema dimensionării stâlpilor la minele de sare din România, Editura Academiei, 1959.